Flow of non-Newtonian fluid in the entrance region of a tube with porous walls

Chen-I Hung and Yeong-Yan Perng
Department of Mechanical Engineering, National Cheng-Kung University, Tainan, Taiwan, ROC

The hydrodynamic development of non-Newtonian fluid flow in the entrance region of a tube with a porous wall is examined numerically by solving the modified Navier–Stokes equations. Cases involving blowing, suction, and no mass transfer through the walls are considered. Velocity distributions, pressure drops, and skin-friction coefficients are presented for each case. A definite concavity is found in the velocity profile near the tube entrance for all cases. Results for Newtonian fluids are compared with previous studies in which boundary-layer theory was used. In the region away from the entrance, it is found that the present results are in good agreement with previous works. In the region close to the entrance, or in the case of suction, boundary-layer theory is shown to be inappropriate.

Keywords: power-law non-Newtonian fluid; entrance region; porous walls; numerical solutions

Introduction

Due to the importance of non-Newtonian fluid in the processing of molten plastics, polymers, etc., considerable research efforts have been conducted to understand the behavior of these fluids. In the flow of a fluid through a tube, the velocity distribution undergoes a development from some initial profile at the inlet to a fully developed profile at locations far downstream. Correspondingly, the pressure gradient in the region of flow development will differ from that of a fully developed flow. Therefore, it is of considerable interest to determine the detailed nature of velocity development in the entrance region.

Numerous papers are found in the literature that deal with analytical, numerical, and experimental studies of entrance flow for non-Newtonian fluids. One of the first analytical solutions for the velocity profiles, obtained by the linearization of the momentum equations, is given by Langhaar[1] for the circular tube. Tiu et al.[2] extended this approach to estimate the loss coefficients in the laminar entrance region for non-Newtonian fluids. Collins and Schowalter[3] employed a perturbation technique to study the flow development of non-Newtonian fluids in a pipe. The Karman–Pohlhausen momentum integral method was first applied to the entrance-region problem by Schiller.[4] Gupta[5] applied a similar approach to the case of pseudoplastic fluids. A variational technique was used by Tomita[6] to investigate the entrance-region flow of power-law fluids at low Reynolds numbers.

A further approach is to obtain numerical solutions by finite-difference techniques. Duda and Vrentas[7] used this method to study the entrance-region flow of a Powell–Eyring non-Newtonian fluid. The inlet region for laminar flow in porous pipes with small rates of injection or suction has been analyzed numerically by Hornbeck et al.[8]

While boundary-layer theory has been extensively used for entrance-flow problems, its assumptions are invalid near the entrance of the tube. Solutions of the full Navier–Stokes equations near the entrance of a tube differ from the boundary-layer solutions. The numerical solutions of the Navier–Stokes equations in the entrance region have been obtained by Wang and Longwell,[9] McDonald et al.,[10] and Koyari et al.;[11] but these authors did not consider blowing or suction, and they did not consider non-Newtonian fluids.

In this article, we investigate the hydrodynamic development of a power-law, non-Newtonian fluid in a circular tube with wall injection and suction. Since the boundary-layer assumptions are not valid in this region, the modified Navier–Stokes equations are solved numerically. The modified equations used for a power-law liquid are different from the conventional Navier–Stokes equations in that the viscosity of a power-law liquid is dependent on the shear rate but the Newtonian viscosity is independent of the shear rate.[12] Results are presented for a Reynolds number of 100. These results are not currently available in the existing literature.

Address reprint requests to Professor Hung at the Department of Mechanical Engineering, National Cheng-Kung University, Tainan, Taiwan 70101, Republic of China.

Received 28 June 1990; accepted 16 December 1990

Analysis

Formulation of problem

Consider steady, laminar isothermal flow of an incompressible non-Newtonian fluid in the entrance region of a circular tube with porous walls. The flow is two-dimensional (2-D) and is uniform at the entrance of the tube. The fluid that is injected in is assumed to be identical to the fluid flowing in the tube.

The geometry being considered is shown in Figure 1. The radius of the tube is r_0 and a cylindrical coordinate system with its origin at the entrance is used. The x-axis is on the tube centerline, and the r-axis is normal to the centerline.

The dimensionless variables chosen are

$$X = x/r_0, \qquad R = r/r_0, \qquad U = u/u_0, \tag{1a}$$

$$V = v/u_0, \qquad P = p/\rho u_0^2 \tag{1b}$$

The corresponding nondimensional governing equations are expressed as follows:

Continuity equation:

$$\partial U/\partial X + 1/R \cdot \partial(RV)/\partial R = 0 \tag{2}$$

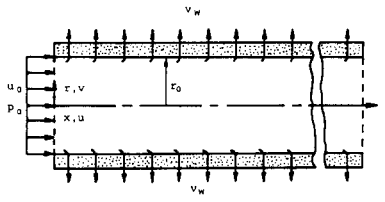

Figure 1 Schematic of the physical situation

X-momentum equation:

$$\partial(UU)/\partial X + 1/R \cdot \partial(RUV)/\partial R = -\partial P/\partial X + 2^n/\mathrm{Re} \cdot [\partial(\eta \cdot \partial U/\partial X)/\partial X + 1/R \cdot \partial(R\eta \cdot \partial U/\partial R)/\partial R] + 2^n/\mathrm{Re} \cdot [\partial(\eta \cdot \partial U/\partial X)/\partial X + 1/R \cdot \partial(R\eta \cdot \partial V/\partial X)/\partial R] \quad (3)$$

R-momentum equation:

$$\partial(UV)/\partial X + 1/R \cdot \partial(RVV)/\partial R = -\partial P/\partial R + 2^n/\mathrm{Re} \cdot [\partial(\eta \cdot \partial V/\partial X)/\partial X + 1/R \cdot \partial(R\eta \cdot \partial V/\partial R)/\partial R] + 2^n/\mathrm{Re} \cdot [\partial(\eta \cdot \partial U/\partial R)/\partial X + 1/R \cdot \partial(R\eta \cdot \partial V/\partial R)/\partial R] \quad (4)$$

where

$$\mathrm{Re} = \rho u_0^{2-n}(2r_0)^n/K, \quad (5a)$$

$$\eta = \{2[(\partial U/\partial X)^2 + (\partial V/\partial R)^2 + (V/R)^2] + (\partial U/\partial R + \partial V/\partial X)^2\}^{(n-1)/2} \quad (5b)$$

Note that for $n=1$, the above system reduces to the conventional Navier–Stokes equations for a Newtonian fluid.

Because of symmetry, only the region between the wall ($R=1$) and the centerline ($R=0$) need to be considered. Nondimensional boundary conditions employed in the present study are described as follows:

Inlet:

$$U=1, \quad V=0 \quad (6a)$$

Walls:

$$U=0, \quad V=Vw \quad (6b)$$

Symmetry axis:

$$\partial U/\partial R=0, \quad V=0 \quad (6c)$$

Condition 6a specifies that the inlet flow is uniform and parallel. In condition 6b, the no-slip condition at the wall and the blowing or suction velocity at the wall are given. For blowing, V_w is defined to be negative; for suction, V_w is positive.

The boundary condition at the exit is different for blowing and suction:[13]

For $V_w > 0$:

$$U=0, \quad \partial V/\partial X=0 \quad (6d)$$

For $Vw \leq 0$:

$$V=0, \quad \partial(U/\bar{U})/\partial X=0 \quad (6e)$$

where $\bar{U}$ represents the average dimensionless axial velocity. Equation 6d represents the case where the fluid inside the tube is taken away continuously through wall suction. The length of computation is taken long enough such that at the exit the fluid is empty there; therefore, the axial velocity is taken as zero and the transverse velocity is treated as invariant in the axial direction. For the wall blowing case, fluid is injected continuously into the tube, and the velocity of fluids inside the tube is increased more and more. For a weak blowing case, the transverse velocity at the exit is much smaller than that in the axial direction. When the flow is fully developed, the axial velocities at exit are linearly proportional to the axial distance; this situation is stated in Equation 6e.

Solution procedure

Because of the elliptic nature of the flow, Equations 2–4 are solved using an implicit finite-difference procedure called SIMPLER (Semi-Implicit Method for Pressure Linked Equations, Revised). This method was developed by Patankar.[14] In this method, the domain is subdivided into a number of control volumes, each associated with a grid point, and the governing differential equations are integrated over each control volume resulting in a system of algebraic equations that can be solved by an iterative technique. All the momentum fluxes across the control surfaces are evaluated approximately by the power-law scheme. To avoid checkerboard fields, the velocities are stored at staggered locations. The pressure–velocity linkage is resolved by a predictor–corrector technique.

In the present method, the Reynolds number is not necessarily restricted to a small value. However, the larger the Reynolds number, the longer is the tube length in order to attain fully developed flow. For the sake of saving computational costs, a Reynolds number of 100 is used in the present study. Also, the entrance length for a power-law fluid is dependent on the flow behavior index n, i.e., the entrance length is longer for a smaller value of n. In this article, the calculations are performed for $n=0.6$, 0.8, 1.0, 1.2, and 1.4. For $n=0.6$, the entrance length is $x/r_0 = 0.2 \cdot \mathrm{Re}$;[3] but for blowing, the computational length should be longer. To ensure that the solutions are not influenced by the outlet boundary conditions, the computational tube length for $V_w < 0$ (blowing) is taken as $40r_0$. For suction ($V_w = 0.02$), the fluid becomes empty at $x/r_0 = 25$;[13] therefore, L is set equal to $25r_0$ in the case of suction.

To determine the appropriate grid size in the x-direction, calculations are performed on increasingly finer grid sizes. The final distribution chosen is a 50×20 nonuniform grid with a denser clustering near the wall and centerline, and near the inlet and exit of the tube. The results of a grid-independency test are presented in Figure 2 in terms of the axial-pressure distribution.

Notation

C_f	Wall skin-friction coefficient
K	Consistency index
L	Length of tube
n	Flow index of power-law fluid
p	Pressure
p_0	Pressure at inlet
r_0	Radius of tube
R	Dimensionless radial coordinate
Re	Reynolds number
u_0	Inlet velocity
u_c	Centerline velocity
U	Dimensionless axial velocity
$\bar{U}$	Average dimensionless axial velocity
V	Dimensionless radial velocity
V_w	Dimensionless wall velocity
X	Dimensionless axial coordinate

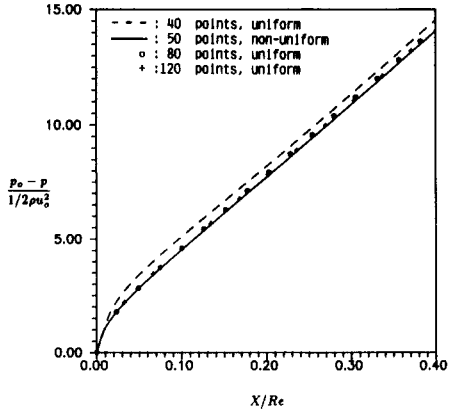

Figure 2 Test of grid-point distribution in axial direction

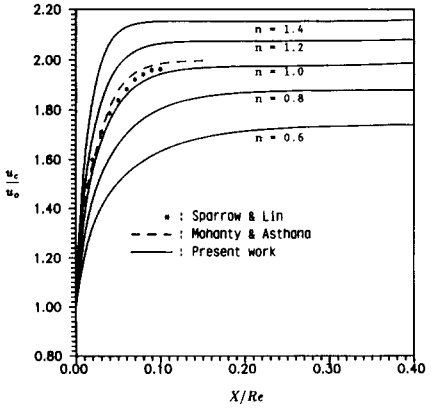

Figure 3 Centerline velocity distribution; $V_w = 0$

Results and discussion

Velocity distribution

In previous studies of entrance-region problems, boundary-layer theory was used extensively. It is known that this approximation is not valid in the vicinity of the entrance of the tube. Figure 3 shows the distributions of the axial velocity at the centerline for a Newtonian fluid, with $V_w = 0$. It is shown that there is a large difference between our solutions and boundary-layer results obtained by Sparrow and Lin[15] and Mohanty and Asthana.[16] Obviously, the axial diffusion term in the momentum equations cannot be neglected in the entrance region. The numerical values obtained from the modified Navier–Stokes solutions must be lesser, as shown in Figure 3.

The velocity gradient near the wall is very large. Therefore, the apparent viscosity of power-law non-Newtonian fluid becomes larger as n is increased. To satisfy the continuity equation, the axial velocity at the tube center should become larger as n increases. Figure 3 also shows this trend. For fully developed flow, the theoretical values of the centerline velocity are given as[17]

$$u_c/u_0 = (3n+1)/(n+1) \tag{7}$$

The above fully developed flow value can be reached only at infinity. The comparison between computational and theoretical values is given in Table 1. The present results are shown to be within 1% of the fully developed flow values.

Figure 4 shows the axial velocity distributions at four different locations for $V_w = 0$. It is seen that there is a noticeable effect upstream of the entrance, and the velocity distribution is concave in the central portion. These velocity "overshoots" have been determined not to be a numerical effect, but rather a valid solution.[13] Also, in Figure 4a, the velocity overshoots are somewhat more obvious for smaller value of n. That is, for a power-law fluid of large flow index n, its apparent viscosity is larger and momentum diffusion near the wall is smaller;

Table 1 Comparison of fully developed centerline velocities

n	$\frac{3n+1}{n+1}$	Present work
0.6	1.75	1.739886
0.8	1.8888	1.879814
1	2.0	1.987861
1.2	2.0909	2.080627
1.4	2.1667	2.158165

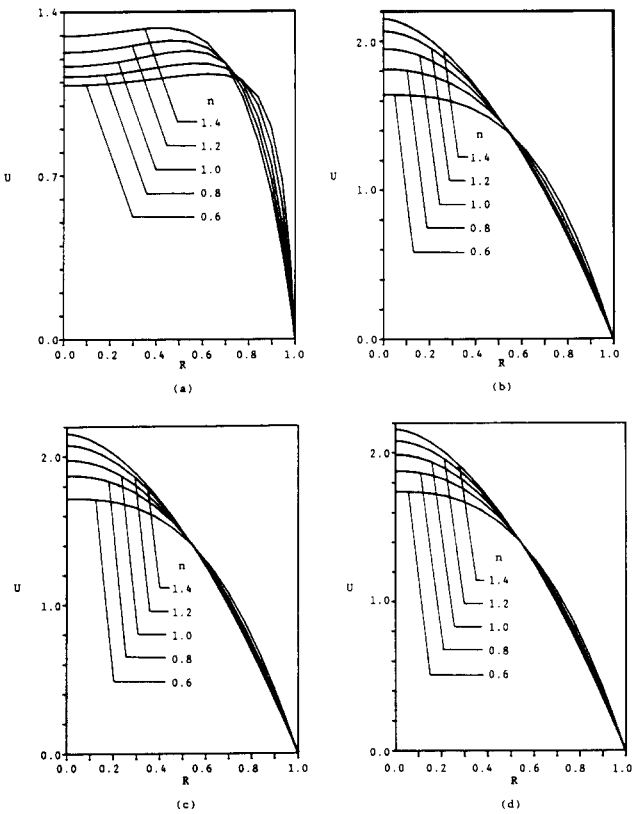

Figure 4 Velocity distributions for $V_w = 0$ at (a) $X/\mathrm{Re} = 0.004364$; (b) $X/\mathrm{Re} = 0.104824$; (c) $X/\mathrm{Re} = 0.201816$; (d) $X/\mathrm{Re} = 0.4$

hence, the concavity of the velocity profile is more obvious. As the length is increased, the viscous effect near the wall is diffused toward the tube center and the concavity of velocity profile disappears gradually. The profiles shown in Figures 4c and 4d are nearly the same. It shows that the computational length taken in the calculations is sufficient to include fully developed flow.

The centerline velocity development with wall blowing ($V_w = -0.02$) is shown in Figure 5. It is found that the centerline velocity increases linearly for $(x/r_0) > 0.12\mathrm{Re}$. This is caused by fully developed flow in this region. Figure 6 presents axial velocity distributions at different axial locations. As before, the concavity of velocity may be noticed by referring to Figures 4a and 6a.

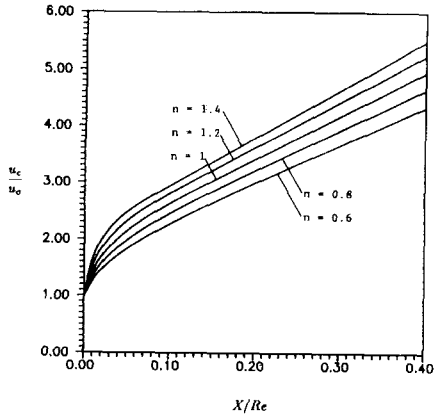

Figure 5 Centerline velocity distribution; $V_w = -0.02$

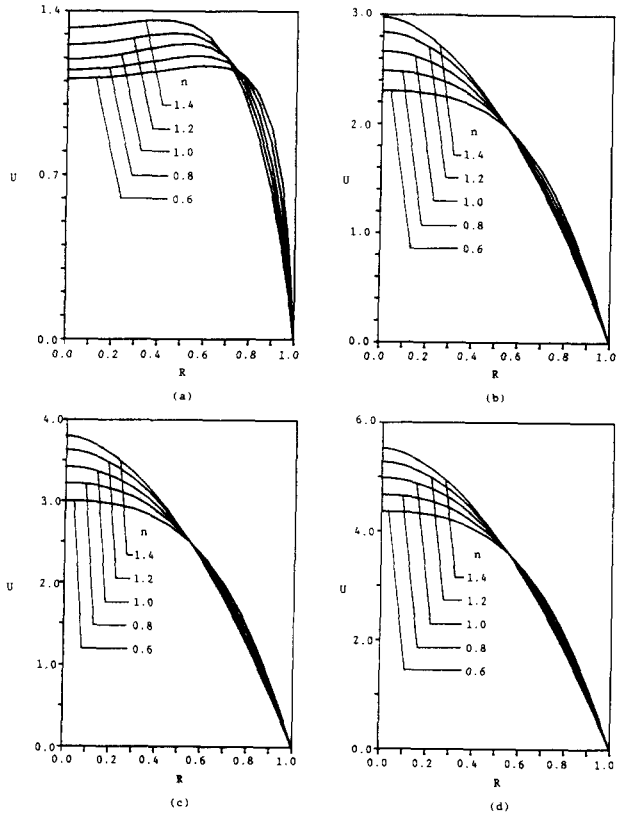

Figure 6 Velocity distributions for $V_w = -0.02$ at (a) $X/\mathrm{Re} = 0.004364$; (b) $X/\mathrm{Re} = 0.104824$; (c) $X/\mathrm{Re} = 0.201816$; (d) $X/\mathrm{Re} = 0.4$

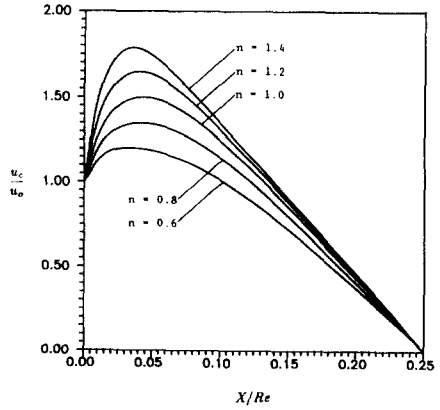

Figure 7 Centerline velocity distribution; $V_w = 0.02$

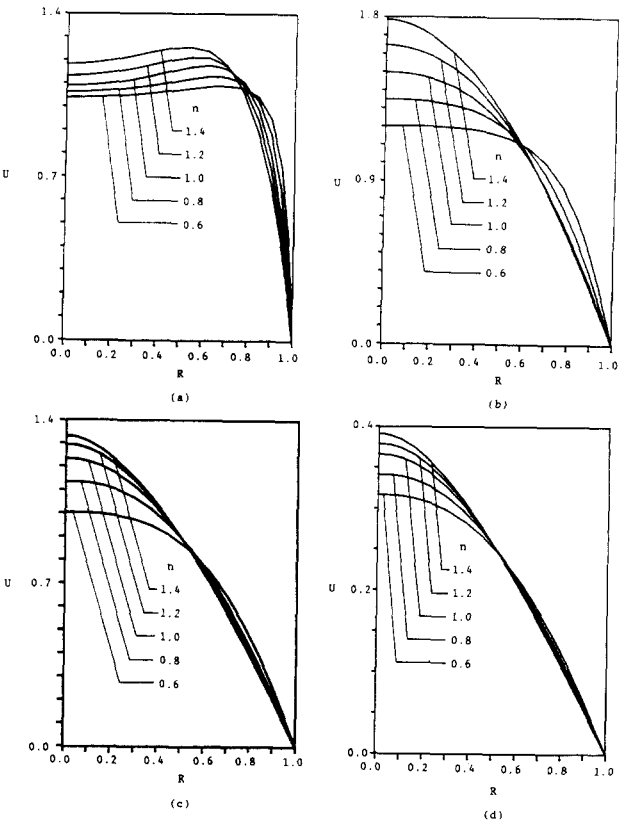

Figure 8 Velocity distributions for $V_w = 0.02$ at (a) $X/\mathrm{Re} = 0.003457$; (b) the locations of maximum centerline velocity; (c) $X/\mathrm{Re} = 0.101386$; (d) $X/\mathrm{Re} = 0.207547$

For the case of wall suction ($V_w = 0.02$), the relatively small amount of fluid being removed gives rise to an increasing centerline velocity in the vicinity of the tube entrance. Thus, the centerline velocity increases to a maximum value, then decreases to zero when the tube is empty. Table 2 lists the axial locations of the maximum centerline velocity, and Figure 7 shows the centerline velocity distribution for various flow index n. It is seen that the maximum value of centerline velocity u_c is increased as n increases, but there is no general rule for the location of maximum u_c.

Figure 8 shows the velocity distributions at various locations for the case of wall suction. In Figure 8a, the concavity of velocity profile still can be found near the leading edge, but the shape is developing until the maximum value is reached (Figure 8b). After that the velocity decreases gradually, because the fluid is removed through the wall, as shown in Figures 8c and 8d.

Compared with the case of an impermeable wall ($V_w = 0$), it can be seen that when the fluid is injected into the tube, the volume of fluid is increased and the fluid near the wall speeds

Table 2 Locations of maximum centerline velocity $V_w = 0.02$

n	$\frac{X}{\mathrm{Re}}$	$\frac{u_c}{u_0}$
0.6	0.035419	1.201076
0.8	0.040013	1.348124
1	0.044754	1.497185
1.2	0.040013	1.646996
1.4	0.035419	1.785425

up in the leading-edge region. Hence, the position of maximum velocity is pushed away from the wall. On the contrary, when fluid is removed from the tube, the fluid slows down and the location of maximum velocity is pulled toward the wall.

Skin-friction coefficient

One of the important tasks in solving the entrance-region problem is the determination of the skin-friction coefficient, which is defined as

$$C_f = \frac{\tau_{rx}}{1/2\rho u_0^2}\bigg|_{r=r_0} \tag{8}$$

Figures 9–11 indicate the distributions of the skin-friction coefficient along the flow direction. In Figure 9, the present solution is compared with a previous study based on an integral solution of the boundary-layer equations.[16] Good agreement is found. Since the skin friction is a local effect near the wall, the momentum integral technique with a higher-order approximation of the velocity profiles can yield accurate results, as shown in Figure 9.

For an impermeable wall (Figure 9), the skin-friction coefficient decreases rapidly to a minimum, and then approaches a constant value. In the case of wall blowing (Figure 10), the volume of fluid inside the tube is increasing; therefore, the skin-friction coefficient decreases first to a minimum, then increases downstream. On the contrary, for wall suction (Figure 11), fluid is removed uniformly from the tube, and the skin-friction coefficient decreases steadily downstream to zero, at which location the fluid is empty.

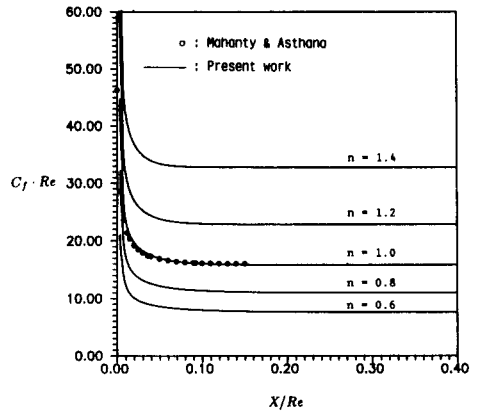

Figure 9 Distributions of skin-friction coefficients; $V_w = 0$

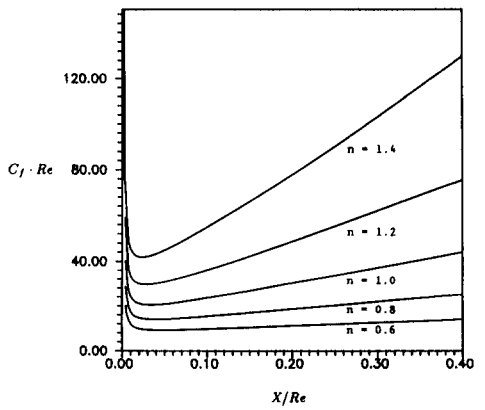

Figure 10 Distributions of skin-friction coefficients; $V_w = -0.02$

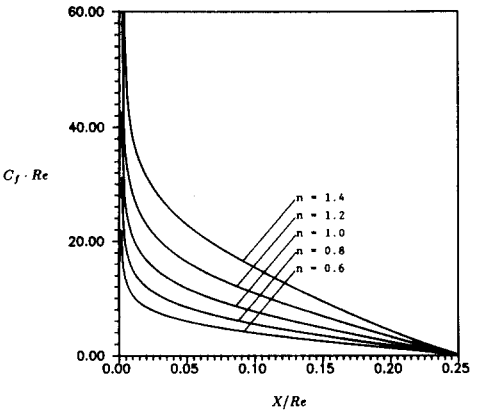

Figure 11 Distributions of skin-friction coefficients; $V_w = 0.02$

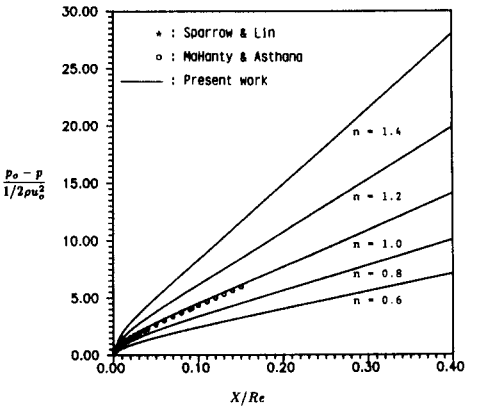

Figure 12 Distributions of pressure drop; $V_w = 0$

Note that, for all cases, a larger value of the flow index n gives rise to a larger skin-friction coefficient. The reason for this phenomenon is because the apparent viscosity of a power-law non-Newtonian fluid is greater for a larger flow index n; therefore, the shear stress at the tube wall is larger for a larger n.

Pressure drop

In the present study, the dimensionless pressure drop is defined as $(p_0 - p)/(1/2 \cdot \rho u_0^2)$, where p and p_0 denote the average pressure at each calculated point and at the inlet section, respectively. The distributions of pressure drop are shown in Figures 12, 13, and 14 for an impermeable wall, wall blowing, and wall suction, respectively.

In Figure 12, the pressure drops for an impermeable wall obtained by Sparrow and Lin[15] and by Mohanty and Asthana[16] are given for comparison. The agreement between the present theory and the previous results is seen to be very good. From the previous discussion, it has been indicated that the centerline velocity is greater for a larger flow index n; therefore, the average momentum at the same cross section will be larger. By the conservation of momentum, a larger pressure drop is needed to maintain the fluid flow.

For wall blowing (Figure 13), as more and more fluid is injected into the tube, the net driving force in the flow direction must be increased continuously. That is, a larger pressure drop is needed to maintain an increased flow rate. The slope of the curve is increased along the flow direction.

Figure 14 is presented for the case of wall suction. To test the validity of the prediction from boundary-layer equations

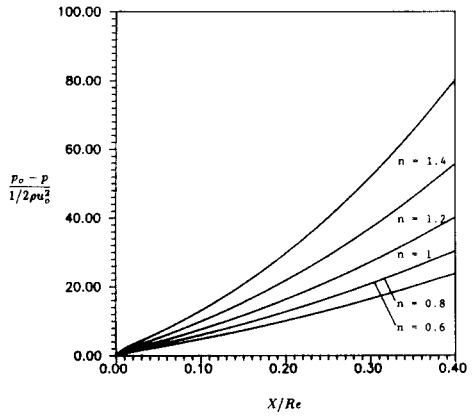

Figure 13 Distributions of pressure drop; $V_w = -0.02$

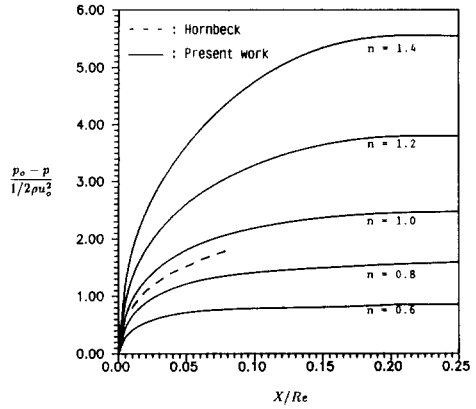

Figure 14 Distributions of pressure drop; $V_w = 0.02$

near the entrance for walls with blowing or suction, the result of Hornbeck et al.[8] is shown for comparison with the present results. The discrepancy is found to be large. The figure clearly shows the necessity of using the modified Navier–Stokes equations for these flow situations. At the exit of the tube, the axial flow velocity is zero; then the gradient of pressure drop is zero, as shown in Figure 14. From the momentum equations, it is known that the loss of momentum should be balanced by the gradients of pressure drop and wall skin friction. This also can be proved from Figures 11 and 14. For wall suction, downstream, the loss of axial momentum is balanced by the gradient of wall skin friction and, therefore, the pressure gradient is zero.

Conclusion

A numerical solution for the flow of a non-Newtonian fluid in the entrance region of a tube with a porous wall has been obtained by solving the modified Navier–Stokes equations. Results for centerline velocity, axial velocity development, skin-friction coefficients, and pressure drop are presented for a Reynolds number of 100. Cases of impermeable wall and wall with blowing or suction have been considered. Comparisons with available results lend support to the findings of the present investigation. The solution of boundary-layer equations is shown not to be valid near the entrance, especially for blowing or suction. A velocity overshoot is found to be present in the near inlet region.

Acknowledgments

The authors wish to thank Professor C. K. Chen, Department of Mechanical Engineering, National Cheng-Kung University, Tainan, Taiwan, ROC and Dr. Win Aung, National Science Foundation, Washington, DC, USA, for helpful discussions and suggestions. The valuable comments given by the reviewers are also very much appreciated.

References

1 Langhaar, H. L. Steady flow in the transition length of a straight tube. *ASME J. Appl. Mech.*, 1942, **9**, 55–58
2 Tiu, C., Boger, D. V., and Halmos, A. L. Generalized method for predicting loss coefficients in entrance region flows for inelastic liquids. *Chem. Eng. J.*, 1972, **4**, 113–117
3 Collins, M. and Schowalter, W. R. Behavior of non-Newtonian fluids in the entry region of a pipe. *AICHE J.*, 1963, **9**, 804–809
4 Schiller, L. Die Entwicklung der laminaren Geschwindigkeits Verteilung und ihre Bedeutung fur Zahigkeitmessungen. *Z. Angew. Math. Mech.*, 1922, **9**, 96–106
5 Gupta, R. C. Entrance region flow of inelastic liquids. *J. Mecanique*, 1969, **8**, 207–214
6 Tomita, Y. Analytical treatments of non-Newtonian fluid flow by introducing the conception of boundary layer. *Bull. JSME*, 1961, **4**, 77–86
7 Duda, J. L. and Vrentas, J. S. Pressure losses in non-Newtonian flows. *Can. J. Chem. Eng.*, 1972, **50**, 671–674
8 Hornbeck, R. W., Rouleau, W. T., and Osterle, F. Laminar entry problem in porous tubes. *Phys. Fluids*, 1963, **6**, 1649–1654
9 Wang, Y. L. and Longwell, P. A. Laminar flow in the inlet section of parallel plates. *AICHE J.*, 1964, **10**, 323–329
10 McDonald, J. W., Denny, V. E., and Mills, A. F. Numerical solutions of the Navier–Stokes equations in inlet regions. *ASME J. Appl. Mech.*, 1972, **39**, 873–878
11 Koyari, Y., Yoshizawa, A., and Takano, A. Studies on the starting flow and inlet flow in a channel and a pipe. *AIAA 14th Fluid and Plasma Dynamics Conf.*, California, 1981, Paper AIAA-81-1221
12 Lenk, R. S. *Polymer Rheology*, Applied Science Publishers, London, 1978
13 Raithby, G. D. and Knudsen, D. C. Hydrodynamic development in a duct with suction and blowing. *ASME J. Appl. Mech.*, 1974, **41**, 896–902
14 Patankar, S. V. *Numerical Heat Transfer and Fluid Flow*, Hemisphere, McGraw-Hill, New York, 1980
15 Sparrow, E. M. and Lin, S. H. Flow development in the hydrodynamic entrance region of tubes and ducts. *Phys. Fluids*, 1964, **7**, 338–347
16 Mohanty, A. K. and Asthana, S. B. L. Laminar flow in the entrance region of a smooth pipe. *J. Fluid Mech.*, 1978, **90**, 433–447
17 Skelland, A. H. P. *Non-Newtonian Flow and Heat Transfer*, John Wiley & Sons, New York, 1967